SCIENTIFIC PROBLEMS
OF MACHINES OPERATION
AND MAINTENANCE
2 (154) 2008

ALEKSANDER MAZURKOW*

The research of the dynamic properties of rotating units in turbochargers

K e y w o r d s

Turbocharger, rotating unit, sliding bearing with a floating ring bearing, rigidity and damping factor.

S ł o w a k l u c z o w e

Turbosprężarka, zespół wirujący, łożysko ślizgowe z panewką pływającą, współczynniki sztywności i tłumienia.

S u m m a r y

The dynamic model of a rotating unit of a turbocharger has been designed. Both masses of the rotors and shaft have been modelled as concentrated masses. The rotating unit has been propped on two supports forming lateral sliding bearings with a floating ring bearing. Each bearing is designed including the floating ring bearing mass. The shaft of a rotating unit spins at angular velocity $\omega_{1;}$ whereas, a floating ring bearing spins at angular speed $\omega_{2.}$ The angular velocity ω_2 has been determined from the equilibrium of friction moments on both the outer and inner surfaces of a floating ring bearing. A mathematical model constitutes a system of differential equations, mutually coupled. The mathematical model has been solved by determining acceleration, velocity and displacement in each node. This work deals with the influence of the imbalance of rotating elements, bearings clearances, rotational speed of a shaft on rigidity and

* Rzeszow University of Technology, The Faculty of Mechanical Engineering and Aeronautics, Departmen of Machine Design, Al. Powstańców Warszawy 8, 35-959 Rzeszów, phone: (017) 865 16 40, fax: (017) 865 11 50, e-mail: algarze@rz.onet.pl

damping factors of bearing supports as well as the amplitude of displacements in nodes of rotating units. Having analysed the results of the research, we noticed the crucial influence of imbalance and a quotient of radial clearances on displacement amplitude in bearing nodes. Also, it has been stated that the growth of quotient of radial clearances causes the growth of displacement amplitude.

1. Introduction

From the point of the generation of oscillation, a turbocharger is a self-generating system. The essential source of oscillations is rotating units [3], [5], [7], [10] with bearings. Because of the simple structure, good dynamic properties [1], [2], [6], [11], and good heat transmission in these types of structures, we use sliding bearings with a floating ring bearing. Good examples are turbochargers installed in engines of cars and fishing boats (Fig.1).

This research deals with the influence of the imbalance of rotating elements, bearing clearances, the rotational speed of a shaft, bearings load on rigidity and damping factors in bearing supports and also displacements amplitude in nodes of the rotating units.

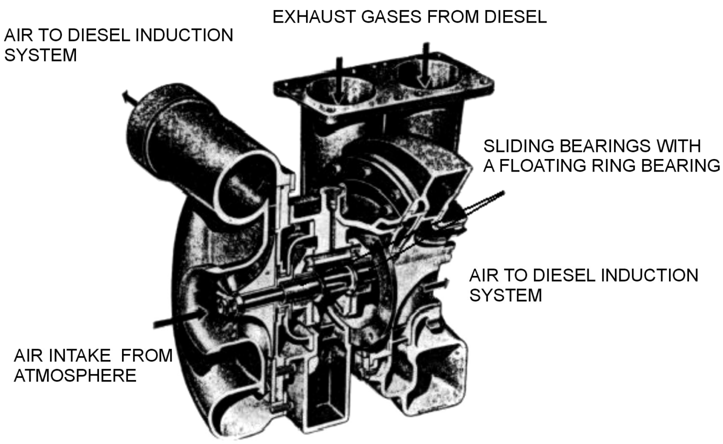

Fig. 1. Section of a C0 -45 turbocharger
Rys. 1. Przekrój turbosprężarki C0-45

2. Dynamic model of rotating unit in a turbocharger

The discussed model of the rotating unit has been described in the Fig.2. In this model, each bearing is modelled including a floating ring bearing mass. Through rigidity and damping factors, oil films capacity towards oscillations damping has been also considered. The motion of the model has been examined in two planes: 0XZ and 0YZ.

Each of rotors with masses distributed in a constant way has been replaced with a concentrated mass found in the center of mass. Thus, a compressor rotor has been replaced with mass m_4 and a turbine rotor with m_1. A distributed mass of a shaft has been replaced with two masses m_2, m_3. Floating ring bearings have masses m_5 and m_6. Shaft sections among supports have been treated as components with constant stiffness E·I. Driving forces, which affect masses m_1 and m_4, constitute either forces of gravity or forces deriving from the imbalance of rotating masses. Having assumed that additional masses m_{n1} and m_{n4} are placed respectively at distances δ_1 and δ_4, the effect of dynamic imbalance [10] has been ignored. The action of each point mass constitutes an outer driving force that equals $m_{n1} \cdot \delta_1 \cdot \omega_1^2$ and $m_{n4} \cdot \delta_4\ w_1^2$. Having assumed that these forces do not act together in a phase, and the angle of displacement phase is represented by φ.

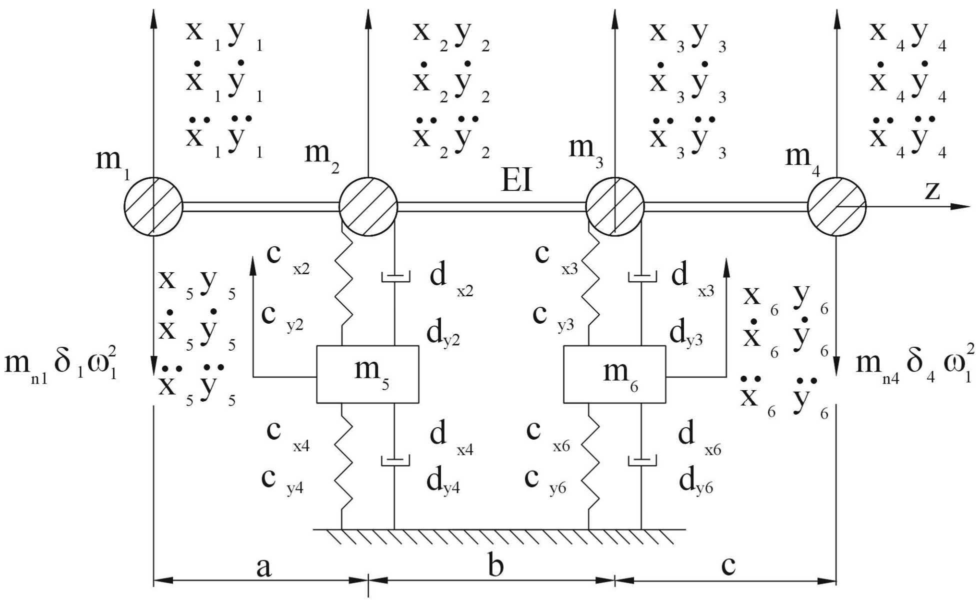

Fig. 2. The model of a rotating unit
Rys. 2. Model zespołu wirującego

3. Mathematical model of a turbocharger rotating unit

Motion equations for the discrete model have been described in Fig. 2 and have been written by the force method for each mass model. In planes 0XZ and 0YZ, these equations are written in the form:

$$
\begin{aligned}
&x_1 = -\alpha_{x11}\left[m_1\ddot{x}_1 - m_{n1}\delta_1\omega^2 \sin \omega t\right] - \alpha_{x12}\left[m_2\ddot{x}_2 + d_{x2}(\dot{x}_2 - \dot{x}_5)\right] - \alpha_{x13}\left[m_3\ddot{x}_3 + d_{x3}(\dot{x}_3 - \dot{x}_6)\right] - \\
&- \alpha_{x14}\left[m_4\ddot{x}_4 - m_{n4}\delta_4\omega^2 \sin \omega t\right]\\
&x_2 = -\alpha_{x21}\left[m_1\ddot{x}_1 - m_{n1}\delta_1\omega^2 \sin \omega t\right] - \alpha_{x22}\left[m_2\ddot{x}_2 + d_{x2}(\dot{x}_2 - \dot{x}_5)\right] - \alpha_{x23}\left[m_3\ddot{x}_3 + d_{x3}(\dot{x}_3 - \dot{x}_6)\right] - \\
&- \alpha_{x24}\left[m_4\ddot{x}_4 - m_{n4}\delta_4\omega^2 \sin \omega t\right]\\
&x_3 = -\alpha_{x31}\left[m_1\ddot{x}_1 - m_{n1}\delta_1\omega^2 \sin \omega t\right] - \alpha_{32}\left[m_2\ddot{x}_2 + d_{x2}(\dot{x}_2 - \dot{x}_5)\right] - \alpha_{x33}\left[m_3\ddot{x}_3 + d_{x3}(\dot{x}_3 - \dot{x}_6)\right] - \\
&- \alpha_{x34}\left[m_4\ddot{x}_4 - m_{n4}\delta_4\omega^2 \sin \omega t\right]\\
&x_4 = -\alpha_{x41}\left[m_1\ddot{x}_1 - m_{n1}\delta_1\omega^2 \sin \omega t\right] - \alpha_{x42}\left[m_2\ddot{x}_2 + d_{x2}(\dot{x}_2 - \dot{x}_5)\right] - \alpha_{x43}\left[m_3\ddot{x}_3 + d_{x3}(\dot{x}_3 - \dot{x}_6)\right] - \\
&- \alpha_{x44}\left[m_4\ddot{x}_4 - m_{n4}\delta_4\omega^2 \sin \omega t\right]\\
&m_5\ddot{x}_5 + c_{x4}x_5 + d_{x4}\dot{x}_5 + c_{x2}(x_5 - x_2) + d_{x2}(\dot{x}_5 - \dot{x}_2) = 0\\
&m_6\ddot{x}_6 + c_{x6}x_6 + d_{x6}\dot{x}_6 + c_{x3}(x_6 - x_3) + d_{x3}(\dot{x}_6 - \dot{x}_3) = 0\\
&y_1 = -\alpha_{x11}\left[m_1\ddot{y}_1 - m_{n1}\delta_1\omega^2 \sin \omega t + Q_1\right] - \alpha_{x12}\left[m_2\ddot{y}_2 + d_{x2}(\dot{y}_2 - \dot{y}_5) + Q_2\right] - \\
&- \alpha_{x13}\left[m_3\ddot{y}_3 + d_{x3}(\ddot{y}_3 - \ddot{y}_6) + Q_3\right] - \alpha_{x14}\left[m_4\ddot{y}_4 - m_{n4}\delta_4\omega^2 \sin \omega t + Q_4\right]\\
&y_2 = -\alpha_{x21}\left[m_1\ddot{y}_1 - m_{n1}\delta_1\omega^2 \sin \omega t + Q_1\right] - \alpha_{x22}\left[m_2\ddot{y}_2 + d_{x2}(\dot{y}_2 - \dot{y}_5) + Q_2\right] - \\
&- \alpha_{x23}\left[m_3\ddot{y}_3 + d_{x3}(\ddot{y}_3 - \ddot{y}_6) + Q_3\right] - \alpha_{x24}\left[m_4\ddot{y}_4 - m_{n4}\delta_4\omega^2 \sin \omega t + Q_4\right]\\
&y_3 = -\alpha_{x31}\left[m_1\ddot{y}_1 - m_{n1}\delta_1\omega^2 \sin \omega t + Q_1\right] - \alpha_{x32}\left[m_2\ddot{y}_2 + d_{x2}(\dot{y}_2 - \dot{y}_5) + Q_2\right] - \\
&- \alpha_{x33}\left[m_3\ddot{y}_3 + d_{x3}(\ddot{y}_3 - \ddot{y}_6) + Q_3\right] - \alpha_{x34}\left[m_4\ddot{y}_4 - m_{n4}\delta\omega^2 \sin \omega t + Q_4\right]\\
&y_4 = -\alpha_{x41}\left[m_1\ddot{y}_1 - m_{n1}\delta_1\omega^2 \sin \omega t + Q_1\right] - \alpha_{x42}\left[m_2\ddot{y}_2 + d_{x2}(\dot{y}_2 - \dot{y}_5) + Q_2\right] - \\
&- \alpha_{x43}\left[m_3\ddot{y}_3 + d_{x3}(\ddot{y}_3 - \ddot{y}_6) + Q_3\right] - \alpha_{x44}\left[m_4\ddot{y}_4 - m_{n4}\delta_4\omega^2 \sin \omega t + Q_4\right]\\
&m_5\ddot{y}_5 + c_{y4}y_5 + d_{y4}\dot{y}_5 + c_{y2}(y_5 - y_2) + d_{y2}(\dot{y}_5 - \dot{y}_2) = Q_5\\
&m_6\ddot{y}_6 + c_{y6}y_6 + d_{y6}\dot{y}_6 + c_{y3}(y_6 - y_3) + d_{y3}(\dot{y}_6 - \dot{y}_3) = Q_6
\end{aligned}
\tag{1}
$$

Whereas, motion equations for the discrete model written as a matrix in planes 0XZ and 0YZ have the form:

$$
\begin{aligned}
&[\mathrm{M_x}]\cdot[\ddot{\mathrm{x}}] + [D_{xx}]\cdot[\dot{\mathrm{x}}] + [D_{xy}]\cdot[\dot{x}] + [C_{xx}]\cdot[\mathrm{x}] + [C_{xy}]\cdot[x] = [\mathrm{F_x(t)}],\\
&[\mathrm{M_y}]\cdot[\ddot{\mathrm{y}}] + [D_{yy}]\cdot[\dot{\mathrm{y}}] + [D_{yx}]\cdot[\dot{\mathrm{y}}] + [C_{yy}]\cdot[\mathrm{y}] + [C_{yx}]\cdot[y] = [\mathrm{F_y(t)}],
\end{aligned}
\tag{2}
$$

The description of particular elements of a matrix of the equation 2 is presented in the work [9]. In the mathematical model of a bearing unit, we have considered impact factors α_{xrs}, α_{yrs} (where; x -defines plane 0XZ, y-defines plane 0YZ, r = 1, 2, 3, 4, s = 1, 2, 3, 4) that are deflections measured in a specific **s**-point, which result from the application of elementary force F=1 [N] in a specific **r-**point Fig. 2.

Impact factors for plane 0XZ are:

$$\alpha_{x11} = \frac{a^2(a+b)}{3EI} + \frac{(a+b)^2}{c_{x2}b^2} + \frac{a^2}{c_{x3}b^2}, \quad \alpha_{x12} = \alpha_{x21} = \frac{a+b}{c_{x2}b}$$

$$\alpha_{x13} = \alpha_{x31} = \frac{-a}{c_{x2}b}, \quad \alpha_{x14} = \alpha_{x41} = \frac{abc}{6EI} - \frac{(a+b)c}{c_{x2}b^2} - \frac{(b+c)a}{c_{x3}b^2},$$

$$\alpha_{x22} = \frac{1}{c_{x2}}, \alpha_{x23} = \alpha_{x32} = 0, \quad \alpha_{x42} = \alpha_{x24} = \frac{-c}{c_{x2}b}, \alpha_{x33} = \frac{1}{c_{x3}}, \tag{3}$$

$$\alpha_{x43} = \alpha_{x34} = \frac{b+c}{c_{x3}b}, \alpha_{x44} = \frac{a^2(b+c)}{3EI} + \frac{(b+c)^2}{c_{x3}b^2} + \frac{c^2}{c_{x2}b^2},$$

For plane 0YZ impact factors $\alpha_{yrs} = \alpha_{ysr}$ by using the substitution $k_{x2} = k_{y2}$, and $k_{x3} = k_{y3}$ we obtain the equation (2).

Substitute rigidity factors (c_{x2}, c_{x3}, c_{x4}, c_{x6}, c_{y2}, c_{y3}, c_{y4}, c_{y6}) and substitute damping factors of oil film (d_{x2}, d_{x3}, d_{x4}, d_{x6}, d_{y2}, d_{y3}, d_{y4}, d_{y6}) for planes 0XZ and 0YZ are equal:

$$c_{x2} = \frac{c_{xx}(1,1)\cdot(x_2 - x_5) + c_{xy}(1,1)\cdot(y_2 - y_5)}{(x_2 - x_5)},$$

$$c_{x3} = \frac{c_{xx}(2,1)\cdot(x_3 - x_6) + c_{xy}(2,1)\cdot(y_3 - y_6)}{(x_3 - x_6)},$$

$$c_{x4} = \frac{c_{xx}(1,2)\cdot x_5 + c_{xy}(1,2)\cdot y_5}{x_5},$$

$$c_{x6} = \frac{c_{xx}(2,2)\cdot x_6 + c_{xy}(2,2)\cdot y_6}{x_6},$$

$$c_{y2} = \frac{c_{yx}(1,1)\cdot(x_2 - x_5) + c_{yy}(1,1)\cdot(y_2 - y_5)}{(y_2 - y_5)},$$

$$c_{y3} = \frac{c_{yx}(2,1)\cdot(x_3 - x_6) + c_{yy}(2,1)\cdot(y_3 - y_6)}{(y_3 - y_6)},$$

$$c_{y4} = \frac{c_{yx}(1,2)\cdot x_5 + c_{yy}(1,2)\cdot y_5}{y_5}, \quad c_{y6} = \frac{c_{yx}(2,2)\cdot x_5 + c_{yy}(2,2)\cdot y_6}{y_6}, \tag{4}$$

$$d_{x3} = \frac{d_{xx}(2,1)\cdot(\dot{x}_3 - \dot{x}_6) + d_{xy}(2,1)\cdot(\dot{y}_3 - \dot{y}_6)}{(\dot{x}_3 - \dot{x}_6)},$$

$$d_{x2} = \frac{d_{xx}(1{,}1)\cdot(\dot{x}_2 - \dot{x}_5) + d_{xy}(1{,}1)\cdot(\dot{y}_2 - \dot{y}_5)}{(\dot{x}_2 - \dot{x}_5)},$$

$$d_{x4} = \frac{d_{xx}(1{,}2)\cdot\dot{x}_5 + d_{xy}(1{,}2)\cdot\dot{y}_5)}{\dot{x}_5},$$

$$d_{x6} = \frac{d_{xx}(2{,}2)\cdot\dot{x}_6 + d_{xy}(2{,}2)\cdot\dot{y}_6}{\dot{x}_6},\quad d_{y3} = \frac{d_{yx}(2{,}1)\cdot(\dot{x}_3 - \dot{x}_6) + d_{yy}(2{,}1)\cdot(\dot{y}_3 - \dot{y}_6)}{(\dot{y}_3 - \dot{y}_6)},$$

$$d_{y2} = \frac{d_{yx}(1{,}1)\cdot(\dot{x}_2 - \dot{x}_5) + d_{yy}(1{,}1)\cdot(\dot{y}_2 - \dot{y}_5)}{(\dot{y}_2 - \dot{y}_5)},$$

$$d_{y4} = \frac{d_{yx}(1{,}2)\cdot\dot{x}_5 + d_{yy}(1{,}2)\cdot\dot{y}_5}{\dot{y}_5},$$

$$d_{y6} = \frac{d_{yx}(2{,}2)\cdot\dot{x}_6 + d_{yy}(2{,}2)\cdot\dot{y}_6}{\dot{y}_6},$$

where: c_{xx}, c_{xy} are rigidity factors of oil film in plane 0XZ,
c_{yx}, c_{yy} are rigidity factors of oil film in plane 0YZ,
d_{xx}, d_{xy} are damping factors of oil film in plane 0XZ,
d_{yx}, d_{yy} are damping factors of oil film in plane 0YZ,

Factors c_{xy}, d_{xy} consider the impact of acting forces in plane 0YZ on displacements in plane 0XZ. While, factors c_{yx}, d_{yx} determine the influence of acting forces in plane 0XZ on displacements in plane 0YZ.

4. Rigidity and damping factors of the sliding bearing with a floating ring bearing

Constructional elements of a bearing are (Fig.3) journal (1), fixed bearing bush (3), and loosely fixed floating ring (2) separating journal and the fixed bearing bush, known as floating ring bearing. The oil is supplied into outer and inner bearing under the pressure through holes (4), which are in fixed bearing bush and floating ring bearing. Circumferential grooves (5) in the fixed bearing bush or floating ring bearing provide regular oil feed to lubricant gaps. Directions of oil flow in a bearing (6).

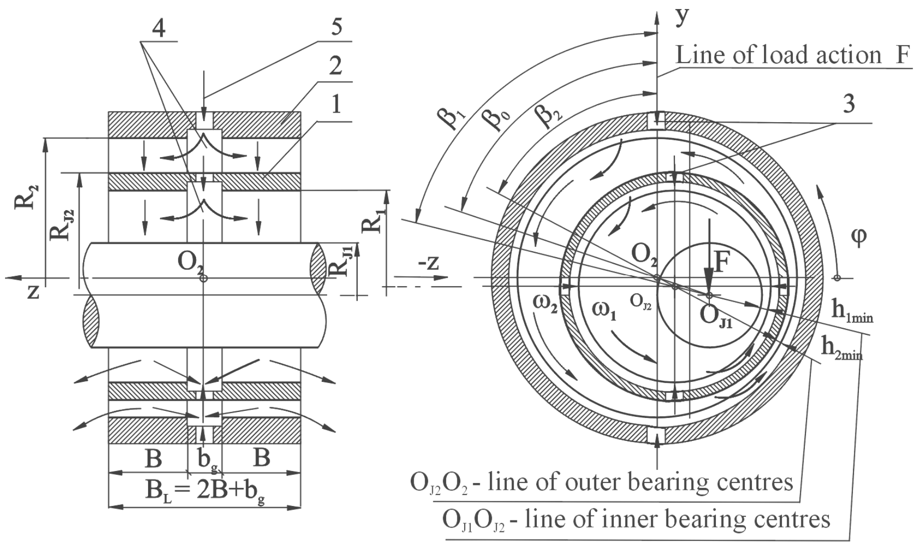

Fig. 3. The sliding bearing with a floating ring bearing
Rys. 3. Łożysko ślizgowe z panewką pływającą

Resultant pressure in oil films and hydrodynamic bearing load capacity (F_L) balances a bearing outer load (F), which is attached to a bearing journal. The isothermal model of a short bearing [4] has been accepted to calculate the work parameters in a static equilibrium. Forces and the moment system are described in Fig. 4.

Work parameters of a bearing are described by forces and moment equations:

Sommerfeld Number for inner oil film $$S_{o1} = \frac{\eta(\omega_1 + \omega_2) \cdot D_1 B}{F} \left(\frac{R_1}{C_{R1}} \right)^2 \quad (5)$$

Sommerfeld Number for outer oil film $$S_{o2} = \frac{\eta \omega_2 D_2 B}{F} \left(\frac{R_3}{C_{R2}} \right)^2 \quad (6)$$

Equations of balance of forces are:

$$\pi \left(\frac{B}{D_2} \right) \cdot S_{01} = \frac{(1-\varepsilon_1^2)^2}{\varepsilon_1 \sqrt{16\varepsilon_1^2 + \pi^2 (1-\varepsilon_1^2)}} \quad (7)$$

$$\pi\left(\frac{B}{D_2}\right)\cdot S_{02}=\frac{(1-\varepsilon_2^2)^2}{\varepsilon_1\sqrt{16\varepsilon_2^2+\pi^2(1-\varepsilon_2^2)}} \tag{8}$$

Equations of the equilibrium of moments on the outer and inner surfaces of a floating ring bearing $M_2(O_{J2})= M_3(O_{J2})$ are:

$$S_{02}\cdot\pi\int_0^{2\pi}\frac{l}{B}\frac{d\varphi_2}{(1+\varepsilon_2\cos\varphi_2)}+\frac{1}{2}\varepsilon_2\cos\beta_2=\left(\frac{C_{R1}}{C_{R2}}\right)\left(\frac{1-\nu}{1-\nu}S_{o1}\pi\int_0^{2\pi}\frac{l}{B}\frac{d\varphi_1}{(1+\varepsilon_1\cos\varphi_1)}-\frac{1}{2}\varepsilon_1\cos\beta_1\right) \tag{9}$$

where

$$\nu=\frac{\omega_2}{\omega_1},\ ctg\beta_1=\frac{\pi\cdot\sqrt{1-\varepsilon_1^2}}{4\cdot\varepsilon_1},\ ctg\beta_2=\frac{\pi\cdot\sqrt{1-\varepsilon_2^2}}{4\cdot\varepsilon_2}, \tag{10}$$

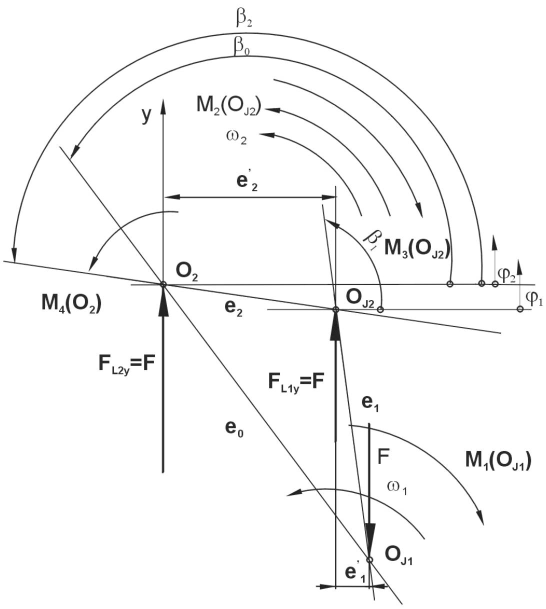

Fig. 4. Forces and moments system in a bearing
Rys. 4. Układ sił i momentów w łożysku

5. Research of dynamic properties

The analysis of dynamic properties of a rotating unit in Fig.1 has been carried out for structural cases described in Chart 1.

Chart 1. Given parameters from calculations of the rotating unit
Tabela1. Parametry zadane od obliczeń zespołu wirującego

Concentrated masses in particular nodes [N·s²/m]					
m_1	m_2	m_3	m_4	m_5	m_6
5.0	0.3	0.25	2.0	0.055	0.055
Bearing loads [N]					
in the second node F = 400, 600			In the third node F = 370, 550		
Radial clearances in bearings [m]					
$C_{R1} = 0.1 \cdot 10^{-3}, 0.17 \cdot 10^{-3}$			$C_{R2} = 0.06 \cdot 10^{-3}, 0.3 \cdot 10^{-3}$		
Journal radiuses for inner bearing and outer bearing [m]					
$R_{J1} = 15.82 \cdot 10^{-3}$[m]			$R_{J1} = 18.89 \cdot 10^{-3}$[m]		
Bearings width [m]					
in the second node B = 0.174			in the third node B = 0.174		
Geometric parameters of rotating unit					
a = 0.055 [m]	b = 0.075 [m]		c = 0.045 [m]	$I_x = 0.15 \cdot 10^{-6}$ [m⁴]	
Material constants					
$E = 1.915 \cdot 10^{11}$[N/m²]			$\eta = 0.028$ [Pa·s]		
Rotational speed of a shaft [rpm]					
N_1=500, 400					
Imbalance of rotating masses [N·s²]					
$N_{w1} = 0.18 \cdot 10^{-4}, 0.88 \cdot 10^{-4}$			$N_{w4} = 0.5 \cdot 10^{-5}, 0.65 \cdot 10^{-4}$		

For the presented given parameters in Chart 1, the following have been determined: rigidity and damping factors in bearings supports and amplitudes and displacement phases as well as acceleration and velocity phases in particular nodes. Moreover, the stability of the rotating unit has been checked. The results are given in Charts 2- 4.

Chart 2. Stiffness and damping factors
Tabela 2. Współczynniki sztywności i tłumienia

Given parameters						
	Task 1	**Task 2**	**Task 3**	**Task 4**	**Task 5**	**Task 6**
[N·s²]	$N_{w1}= 0.18 \cdot 10^{-4}$	$N_{w1}= 0.18 \cdot 10^{-4}$	$N_{w1}= 0.18 \cdot 10^{-4}$	$N_{w1}= 0.18 \cdot 10^{-4}$	$N_{w1}= 0.18 \cdot 10^{-4}$	$N_{w1}= 0.88 \cdot 10^{-4}$
[N·s²]	$N_{w2}= 0.5 \cdot 10^{-5}$	$N_{w2}= 0.5 \cdot 10^{-5}$	$N_{w2}= 0.5 \cdot 10^{-5}$	$N_{w2}= 0.5 \cdot 10^{-5}$	$N_{w2}= 0.5 \cdot 10^{-5}$	$N_{w2}= 0.5 \cdot 10^{-5}$
[rpm]	N_1=500	N_1=500	N_1=400	N_1=500	N_1=500	N_1=400
[N]	in the second node F=400	in the second node F=600	in the second node F=400	In the second node F=400	in the second node F=400	in the second node F=400
[N]	in the third node F=370	in the third node F= 550	in the third node F=370	In the third node F=370	in the third node F=370	in the third node F=370
[m]	$C_{R1}= 0.1 \cdot 10^{-3}$	$C_{R1}= 0.1 \cdot 10^{-3}$	$C_{R1}= 0.1 \cdot 10^{-3}$	$C_{R1}= 0.17 \cdot 10^{-3}$	$C_{R1}= 0.1 \cdot 10^{-3}$	$C_{R1}= 0.1 \cdot 10^{-3}$
[m]	$C_{R2}= 0.06 \cdot 10^{-3}$	$C_{R2}= 0.06 \cdot 10^{-3}$	$C_{R2}= 0.06 \cdot 10^{-3}$	$C_{R2}= 0.06 \cdot 10^{-3}$	$C_{R2}= 0.3 \cdot 10^{-3}$	$C_{R2}= 0.06 \cdot 10^{-3}$

Given parameters						
	Task 1	**Task 2**	**Task 3**	**Task 4**	**Task 5**	**Task 6**
Stiffness and damping factors: J=1, I=1						
b_{xx} [N·s/m]	4520	10320	8765	4297	6468	8765
b_{xy} [N·s/m]	2415	3514	2970	1368	2071	2970
b_{yx} [N·s/m]	2415	3514	2970	1368	2071	2970
b_{yy} [N·s/m]	7301	5118	4819	1393	4340	4819
k_{xx}[N/m]	$8.718 \cdot 10^{6}$	$1.6335 \cdot 10^{7}$	$9.838 \cdot 10^{6}$	$9.633 \cdot 10^{6}$	$8.014 \cdot 10^{6}$	$9.838 \cdot 10^{6}$
k_{xy} [N/m]	$1.632 \cdot 10^{7}$	$2.382 \cdot 10^{7}$	$1.597 \cdot 10^{7}$	$9.807 \cdot 10^{6}$	$1.68 \cdot 10^{7}$	$1.597 \cdot 10^{7}$
k_{yx} [N/m]	$-6.735 \cdot 10^{6}$	$-6.113 \cdot 10^{6}$	$-5.162 \cdot 10^{6}$	$-5.957 \cdot 10^{5}$	$-8.113 \cdot 10^{6}$	$-5.162 \cdot 10^{6}$
k_{yy} [N/m]	$9.328 \cdot 10^{6}$	$1.343 \cdot 10^{7}$	$9.126 \cdot 10^{6}$	$4.891 \cdot 10^{6}$	$9.469 \cdot 10^{6}$	$9.126 \cdot 10^{6}$
Stiffness and damping factors: J=1, I=2						
b_{xx} [N·s/m]	58560	89540	73510	85210	8061	7351
b_{xy} [N·s/m]	19930	29550	24740	28280	1703	24740
b_{yx} [N·s/m]	19930	29550	24740	28280	1703	24740
b_{yy} [N·s/m]	28660	33910	31300	33230	875.1	31300
k_{xx}[N/m]	$1.84 \cdot 10^{7}$	$3.535 \cdot 10^{7}$	$2.107 \cdot 10^{7}$	$2.292 \cdot 10^{7}$	$1.508 \cdot 10^{7}$	$2.107 \cdot 10^{7}$
k_{xy} [N/m]	$2.647 \cdot 10^{7}$	$4.057 \cdot 10^{7}$	$2.666 \cdot 10^{7}$	$2.693 \cdot 10^{7}$	$7.753 \cdot 10^{6}$	$2.666 \cdot 10^{7}$
k_{yx} [N/m]	$-6.588 \cdot 10^{6}$	$-4.887 \cdot 10^{6}$	$-4.636 \cdot 10^{6}$	$-3.582 \cdot 10^{6}$	$-1.193 \cdot 10^{6}$	$-4.636 \cdot 10^{6}$
k_{yy} [N/m]	$1.489 \cdot 10^{6}$	$2.134 \cdot 10^{7}$	$1.452 \cdot 10^{7}$	$1.43 \cdot 10^{7}$	$2.405 \cdot 10^{6}$	$1.452 \cdot 10^{7}$
Stiffness and damping factors: J=2, I=1						
b_{xx} [N·s/m]	6885	9533	73510	3952	6126	8204
b_{xy} [N·s/m]	2247	3243	24740	1273	1920	2763
b_{yx} [N·s/m]	2247	3243	24740	1273	1920	2763
b_{yy} [N·s/m]	4431	4969	31300	1343	4264	4707
k_{xx}[N/m]	$7.745 \cdot 10^{6}$	$1.427 \cdot 10^{7}$	$8.717 \cdot 10^{6}$	$2.292 \cdot 10^{7}$	$7.13 \cdot 10^{6}$	$8.817 \cdot 10^{6}$
k_{xy} [N/m]	$1.528 \cdot 10^{7}$	$2.186 \cdot 10^{7}$	$1.485 \cdot 10^{7}$	$2.693 \cdot 10^{7}$	$1.583 \cdot 10^{7}$	$1.485 \cdot 10^{7}$
k_{yx} [N/m]	$-6.808 \cdot 10^{6}$	$-6.289 \cdot 10^{6}$	$-5.252 \cdot 10^{6}$	$-3.582 \cdot 10^{6}$	$-8.2 \cdot 10^{6}$	$-5.252 \cdot 10^{6}$
k_{yy} [N/m]	$8.691 \cdot 10^{6}$	$1.243 \cdot 10^{7}$	$8.508 \cdot 10^{6}$	$1.43 \cdot 10^{7}$	$8.818 \cdot 10^{6}$	$8.508 \cdot 10^{6}$
Stiffness and damping factors: J=2, I=2						
b_{xx} [N·s/m]	54320	81400	67760	78390	7241	67760
b_{xy} [N·s/m]	18490	27140	22940	26240	1563	22940
b_{yx} [N·s/m]	18490	27140	22940	26240	1563	22940
b_{yy} [N·s/m]	27870	32610	30320	32120	826.6	30320
k_{xx}[N/m]	$1.625 \cdot 10^{7}$	$3.072 \cdot 10^{7}$	$1.859 \cdot 10^{7}$	$2.023 \cdot 10^{7}$	$1.331 \cdot 10^{7}$	$1.859 \cdot 10^{7}$
k_{xy} [N/m]	$2.45 \cdot 10^{7}$	$3.691 \cdot 10^{7}$	$2.457 \cdot 10^{7}$	$2.476 \cdot 10^{7}$	$7.037 \cdot 10^{6}$	$2.457 \cdot 10^{7}$
k_{yx} [N/m]	$-6.801 \cdot 10^{6}$	$-5.354 \cdot 10^{6}$	$-4.885 \cdot 10^{6}$	$-3.848 \cdot 10^{6}$	$-1.047 \cdot 10^{6}$	$-4.885 \cdot 10^{6}$
k_{yy} [N/m]	$1.389 \cdot 10^{7}$	$1.975 \cdot 10^{7}$	$1.355 \cdot 10^{7}$	$1.334 \cdot 10^{7}$	$2.235 \cdot 10^{6}$	$1.355 \cdot 10^{7}$
Stability research of rotating unit						
	unstable	stable	stable	stable	stable	stable

Chart 3. The influence of rotors imbalance on displacement amplitude in nodes of rotating unit
Tabela 3. Wpływ niewyważenia wirników na amplitudę przemieszczeń w węzłach zespołu wirującego

	Displacement amplitude in nodes of rotating unit [m]					
	x_1	x_2	x_3	x_4	$\mathbf{x_5}$	$\mathbf{x_6}$
	y_1	y_2	y_3	y_4	$\mathbf{y_5}$	$\mathbf{y_6}$
Task 3	$2.267 \cdot 10^{-6}$	$1.266 \cdot 10^{-6}$	$1.162 \cdot 10^{-6}$	$2.344 \cdot 10^{-6}$	**$0.2682 \cdot 10^{-6}$**	**$0.2351 \cdot 10^{-6}$**
Task 6	$6.908 \cdot 10^{-6}$	$6.19 \cdot 10^{-6}$	$8.431 \cdot 10^{-6}$	$13.16 \cdot 10^{-6}$	**$1.577 \cdot 10^{-6}$**	**$2.076 \cdot 10^{-6}$**
Task 3	$3.641 \cdot 10^{-6}$	$3.185 \cdot 10^{-6}$	$2.971 \cdot 10^{-6}$	$3.203 \cdot 10^{-6}$	**$0.5455 \cdot 10^{-6}$**	**$0.3799 \cdot 10^{-6}$**
Task 6	$17.63 \cdot 10^{-6}$	$22.04 \cdot 10^{-6}$	$29.43 \cdot 10^{-6}$	$34.82 \cdot 10^{-6}$	**$3.441 \cdot 10^{-6}$**	**$4.067 \cdot 10^{-6}$**

Chart 4. The influence of radial clearances on displacement amplitude in nodes of rotating unit
Tabela 4. Wpływ luzów promieniowych na amplitudę przemieszczeń w węzłach zespołu wirującego

	Displacement amplitude in nodes of rotating unit [m]					
	x_1	x_2	x_3	x_4	$\mathbf{x_5}$	$\mathbf{x_6}$
	y_1	y_2	y_3	y_4	$\mathbf{y_5}$	$\mathbf{y_6}$
Task 2	$2.33\cdot10^{-6}$	$1.437\cdot10^{-6}$	$1.445\cdot10^{-6}$	$2.785\cdot10^{-6}$	$\mathbf{0.2872\cdot10^{-6}}$	$\mathbf{0.2733\cdot10^{-6}}$
Task 4	$3.277\cdot10^{-6}$	$2.838\cdot10^{-6}$	$2.645\cdot10^{-6}$	$3.03\cdot10^{-6}$	$\mathbf{0.2636\cdot10^{-6}}$	$\mathbf{0.2508\cdot10^{-6}}$
Task 5	$3.557\cdot10^{-6}$	$3.196\cdot10^{-6}$	$2.86\cdot10^{-6}$	$2.85\cdot10^{-6}$	$\mathbf{1.43610^{-6}}$	$\mathbf{1.228\cdot10^{-6}}$
Task 2	$3.745\cdot10^{-6}$	$3.3\cdot10^{-6}$	$3.096\cdot10^{-6}$	$3.35\cdot10^{-6}$	$\mathbf{0.5687\cdot10^{-6}}$	$\mathbf{0.3973\cdot10^{-6}}$
Task 4	$3.816\cdot10^{-6}$	$3.509\cdot10^{-6}$	$3.219\cdot10^{-6}$	$3.14\cdot10^{-6}$	$\mathbf{0.2088\cdot10^{-6}}$	$\mathbf{0.1646\cdot10^{-6}}$
Task 5	$3.606\cdot10^{-6}$	$3.264\cdot10^{-6}$	$2.806\cdot10^{-6}$	$2.54\cdot10^{-6}$	$\mathbf{3.88\cdot10^{-6}}$	$\mathbf{3.265\cdot10^{-6}}$

Conclusions

The case study of a rotating unit running at high rotating speed (n=400 – 500 rpm) and under light load F= <370 – 600> [N] has been considered. The analysis of the research results indicates the following:

- Structural sample No1 is the unstable example. The stability of a rotating units (structural tasks 2, 3, 4, 5, 6) has been achieved due to the boost in bearings load, the reduction in rotational speed of a shaft, and the boost of radial clearances.
- The value of rotors' imbalance (Tasks 1 -6) has an essential influence on oscillation level. The amplitude of displacements (Chart 3) in the node 4 for a coordinate y_4 has increased by 11 times.
- The rapid growth in the value of the quotient of radial clearances causes the growth of displacements amplitude in nodes (5 and 6) which form bearings supports.

The concluding remarks are as follows:

- A journal bearing geometry has a significant impact on the amplitude of displacements in the bearing nodes and, in consequence, on the proper operation of a turbocharger,
- The imbalance of rotating masses has an unfavourable influence on the vibration level of the rotating unit of a turbocharger.

References

[1] Domes B., Amplituden der Unwucht – und Selbsterregen Schwingungen Hochtouriger mit Rotierenden und nichtrotierenden Schwimmenden Büchsen, Diss. Universität Karlsruhe 1980.

[2] Dong X., Zhao Z., Experimental and Analytical research on Floating – Ring Bearings for Engine, Applications. Trans. ASME – J. Of Tribology, January 1990, vol 112/119.

[3] Feuchte B., Biegeschwingungen an Rotorem von Kreiselpumpen und Kreiselverichtern In hydrodynamischen Gleitlagern, Maschbau-tech. 1987 t. 36, nr 3.
[4] Kaniewski W., Warunki diatermicznego filmu smarnego, Zeszyty naukowe Politechniki Łódzkiej, Zeszyt specjalny, z.14,1977.
[5] Kiciński J.: Dynamika wirników i łożysk ślizgowych. Instytut Maszyn Przepływowych im. R. Szewalskiego PAN, tom 28. Gdańsk 2005.
[6] Krause R., Experimentelle Untersuchung eines dynamisch beanspruchten Schwimmbüchsenlagers, ETH Zürich, 1987 r.
[7] Lund J.W., Review of the conspect of dynamic coefficients for fluid film journal bearings, Trans. ASME – J.Tribol. 1987 t.109, nr 1.
[8] Mazurkow A., Termodynamiczna teoria smarowania i statyczne charakterystyki ślizgowego łożyska poprzecznego z panewką pływającą, Praca doktorska, Politechnika Rzeszowska, 1993.
[9] Mazurkow A., Niepublikowane materiały Katedry Konstrukcji Maszyn Politechniki Rzeszowskiej, Rzeszów 2007.
[10] Muszyńska A., Modelowanie wirników, IV kurs szkoleniowy z cyklu Dynamika Maszyn, Jabłonna 5-10 listopada 1979 r.
[11] Spiegel Klaus, Fricke Jürgen. Bemessungs -und Gestaltungsregeln für Gleitlager: Anlagewinkel, An- und Auslauf, Beanspruchung der Gleitflächen. Gesellschaft für Tribologie e.V. Reibung, Schmierung und Verschleiß. Göttingen, 2006.

Manuscript received by Editorial Board, July 01, 2008

Badanie właściwości dynamicznych zespołów wirujących turbosprężarek

S t r e s z c z e n i e

Opracowano model dynamiczny zespołu wirującego turbosprężarki. Masę wirników i wału zamodelowano jako masy skupione. Zespół wirujący został podparty na dwóch podporach stanowiących poprzeczne łożyska ślizgowe z panewką pływającą. Każde łożysko zamodelowano uwzględniając masę panewki pływającej. Wał zespołu wirującego obraca się z prędkością kątową ω_1, natomiast panewka pływająca z prędkością kątową ω_2. Prędkość kątowa ω_2 wyznaczona została z równowagi momentów tarcia na powierzchni zewnętrznej i wewnętrznej panewki pływającej. Model matematyczny stanowi układ równań różniczkowych, wzajemnie sprzężonych. Model matematyczny rozwiązano wyznaczając w każdym węźle: przyśpieszenie, prędkości i przemieszczenia. W pracy przedstawiono wpływ: niewyważenia elementów wirujących, luzów łożyskowych, prędkości obrotowej wału na współczynniki sztywności i tłumienia podpór łożyskowych oraz amplitudę przemieszczeń węzłów zespołu wirującego. Analizując wyniki badań stwierdzono wpływ niewyważenia i ilorazu luzów promieniowych na amplitudę przemieszczeń w węzłach łożyskowych. Ze wzrostem ilorazu luzów promieniowych i niewyważenia rosną amplitudy przemieszczeń.